iJRASET
International Journal For Research in
Applied Science and Engineering Technology

INTERNATIONAL JOURNAL FOR RESEARCH
IN APPLIED SCIENCE & ENGINEERING TECHNOLOGY

Volume: 14 Issue: VII Month of publication: July 2026

DOI: https://doi.org/10.22214/ijraset.2026.84327

International Journal for Research in Applied Science & Engineering Technology (IJRASET)
ISSN: 2321-9653; IC Value: 45.98; SJ Impact Factor: 7.538
Volume 14 Issue VII July 2026- Available at www.ijraset.com

Design of an Improved Physics-Aware Early-Life Prognostic Framework for Reliable Remaining Useful Life Prediction of Lithium-Ion Batteries in Real-Time Battery Management Systems

Vinaya Sonparote
TGPCET, Nagpur

Abstract: Unanticipated lithium-ion battery RUL deterioration creates economic loss, reliability issues, and safety hazards in electric mobility, grid-scale storage, and safety-critical cyber-physical systems. Data-driven prognostics has improved, but early-life prediction, physical interpretability of learnt representations, and real-time Battery Management System (BMS) deployability remain difficult challenges. Many models rely on raw voltage, current, and temperature inputs drawn from a large share of battery lifespan data, but deep learning approaches show unstable generalization and opaque decision mechanisms when operating conditions differ from training regimens.

To address these issues, this study introduces a physics-aware and learning-driven prognostic system that uses degradation saliency analysis, constrained feature representation, early-life inference, and real-time validation. Cycle-Resolved Thermo-Electrochemical Saliency Decomposition (CR-TESD) decomposes charge–discharge cycles into phase-aware degradation saliency maps, revealing aging-relevant information even in early operating phases. For compact, physically consistent health trajectories, the Physics-Anchored Feature Manifold Compression Network (PA-FMCN) embeds saliency-weighted features and applies electrochemical admissibility and monotonic aging constraints during latent-space construction. The Progressive Early-Life RUL Bootstrap Learner (PEL-RBL) estimates RUL with limited lifespan data by gradually aligning early degradation traits with end-of-life patterns. For robustness and interpretability, the Physics-Guided Temporal Hybrid Prognostic Network (PG-THPN) refines long-term temporal dependencies and nonlinear deterioration dynamics using GRU–CNN temporal learning combined with physics-derived degradation states. Finally, the BMS-Aware Scalability and Trust Validation Framework (BMS-STVF) evaluates computational efficiency, latency, and consistency under streaming BMS constraints for real-world application.

Early-life RUL accuracy, generalization stability, and inference efficiency outperform machine learning and deep learning baselines on benchmark battery aging datasets. The methodology improves battery prognostics beyond predictive performance by providing physically grounded, uncertainty-aware, deployment-ready RUL estimates for next-generation intelligent BMS and proactive energy system management.

Keywords: Battery Prognostics; Remaining Useful Life Prediction; Physics-Aware Machine Learning; Early-Life Degradation Analysis; Battery Management Systems.

I. INTRODUCTION

High energy density, prolonged cycle life, and favorable power characteristics make lithium-ion batteries the preferred energy storage option in electric vehicles, renewable energy integration, aerospace systems, and portable electronics. Battery-powered systems are safety-critical and cost-sensitive; therefore, precise RUL estimates are crucial for dependability, preventative maintenance, and lifetime optimization. Battery prognostics is a scientific and industrial concern because RUL prediction influences operational scheduling, warranty assessment, safety monitoring, and second-life use.

Traditional battery health prediction methods used physics-based electrochemical modeling, equivalent circuit representations, empirical degradation equations, and laboratory-determined parameters. These models are interpretable, but they require calibration, material expertise, and assumptions that do not generalize across all chemistries, operating conditions, or aging trajectories. Physics-driven methods cannot capture nonlinear and data-dependent degradation events caused by variable load profiles, environmental stress, and manufacturing abnormalities.

Data-driven and machine-learning-based prognostic methods have emerged to address these issues. Support Vector Machines, Random Forests, Gaussian Process Regression, and more recently LSTM and convolutional neural networks have shown high predictive capability on large deterioration datasets. Despite empirical success, these methods have fundamental disadvantages. Most models restrict early-life screening and proactive quality evaluation by relying on features drawn from a large portion of the battery lifespan. The learned representations are often opaque, limiting physical insight into degradation causes and affecting deployment dependability.

A further key issue is the disconnect between model accuracy and deployability. Real-time Battery Management Systems cannot use high-capacity deep learning models due to computational complexity, memory footprint, and inference delay. Many approaches also separate feature extraction, learning, assessment, and deployment into disjoint stages. This fragmented architecture affects robustness, interpretability, and scalability in scenarios with unpredictable operational regimes or constrained hardware.

Experimental hybrid prognostic methods that combine physics-based insight with learning-driven models are being explored. Most hybrid strategies embed physical constraints only at the model-output level or employ simplified degradation cues, missing opportunities to integrate electrochemical information into feature representation, temporal learning, and validation. A unified framework for early-life RUL prediction, uncertainty quantification, and BMS-aware validation is therefore needed. This paper proposes an end-to-end, physics-aware, deployment-oriented RUL prediction paradigm for battery prognostics that prioritizes degradation saliency discovery, physically admissible representation learning, early-life inference, hybrid temporal modeling, and real-time validation over predictive accuracy alone. These components are tightly integrated into a single analytical pipeline to address long-standing interpretability, robustness, and operational feasibility challenges, turning battery RUL estimation into a solid decision-support capability rather than a black-box prediction task.

A. Motivation and Contributions

The growing gap between battery prognostic model sophistication and energy-system utility drives this research. Recent machine learning and deep learning models offer high accuracy but rely on late-life deterioration data, lack physical grounding, and fail to meet Battery Management System computational and reliability criteria. This separation limits their use in early problem identification, safety assurance, and lifetime cost minimization. An inaccurate early-life RUL forecast impairs proactive maintenance, incoming quality screening, and risk-aware operational planning. A new technique that combines data-driven adaptation with electrochemical realism is needed to scale across datasets and operating conditions.

This research proposes a unified prognostic strategy that redefines battery RUL estimation as a multi-stage analytical process rather than a single prediction model. It begins with Cycle-Resolved Thermo-Electrochemical Saliency Decomposition to identify charging-phase and early-cycle degradation-relevant signal regions. Next, the Physics-Anchored Feature Manifold Compression Network embeds aging data into an electrochemical-admissibility-controlled compact latent space, yielding physically meaningful deterioration paths. On this basis, the Progressive Early-Life RUL Bootstrap Learner estimates RUL from limited lifespan data by aligning early deterioration signals with end-of-life trends. A Physics-Guided Temporal Hybrid Prognostic Network blends GRU–CNN temporal learning with physics-derived degradation stages for robustness and interpretability. Finally, the BMS-Aware Scalability and Trust Validation Framework evaluates computing efficiency, inference delay, and consistency to enable real-time deployment. Together, these advances enhance early-life predictability, physical interpretability, predictive accuracy, and deployment readiness, providing a scalable and dependable platform for next-generation intelligent Battery Management Systems.

II. REVIEW OF EXISTING MODELS USED FOR ANALYSIS

The rise of electric vehicles, grid-scale storage, and safety-critical cyber-physical systems has accelerated lithium-ion battery useful-life prediction research over the last two years. Recent research suggests a move from single-model, feature-centric approaches toward hybrid, multi-stage, physics-informed learning. Pratheeba and Sukumar's hybrid HGRN–SCSO approach [1] showed that long-term degradation learning benefits from heuristic optimization combined with recurrent structures. Similar deep-learning-driven optimization approaches by Iftikhar et al. [2] focused on end-to-end feature learning but implicitly depend on large data volumes and stable operating conditions. Further research focused on progressive learning and decomposition-based representations for non-stationary aging: Ibrahim et al. [4] optimized hybrid pipelines for limited-sample situations, while Wang et al. [3] reduced noise accumulation using multivariate Mamba topologies with adaptive SVD. Multi-scale, jump-connection CNNs [5] and attention-guided CNN-BiLSTM structures [6] further popularized convolutional architectures.

Table 1. Empirical Review of Existing Models

Ref.	Method	Main Objectives	Findings	Limitations
[1]	Hybrid HGRN–SCSO	Improve RUL prediction accuracy using hybrid recurrent networks with swarm optimization	Demonstrated improved convergence stability and reduced prediction error under EV operating profiles	Optimization-heavy structure increases computational complexity and limits real-time deployment
[2]	Deep Learning Optimization Framework	End-to-end RUL learning using deep neural architectures	Achieved improved accuracy over traditional ML models on benchmark datasets	Performance strongly dependent on large training datasets and lacks physical interpretability
[3]	Progressive Mamba + Adaptive SVD	Address non-stationary degradation through progressive residual learning	Effectively suppressed noise accumulation and improved long-horizon prediction accuracy	Model complexity and limited interpretability of learned residuals
[4]	Hybrid Optimized RUL Framework	Enable reliable RUL prediction with limited data samples	Showed robustness under data scarcity and improved early prediction capability	Requires careful tuning of optimization parameters for stability
[5]	Jump-Connection Multi-Scale CNN	Capture degradation patterns at multiple temporal scales	Improved feature extraction and accuracy in mid-to-late lifecycle stages	Weak early-life prediction and high computational cost
[6]	AT-CNN-BiLSTM	Joint SoH estimation and RUL prediction using attention-guided temporal learning	Enhanced temporal dependency modeling and improved RUL accuracy	Attention mechanism increases inference latency
[7]	MWASFormer	Model long-range dependencies using transformer-based architecture	Achieved strong performance on long-cycle datasets	High memory requirements and limited suitability for embedded systems
[8]	CEEMDAN + BILSTM–MHA	Separate intrinsic degradation modes before temporal learning	Improved prediction stability and robustness against noise	Multi-stage preprocessing increases pipeline complexity
[9]	ICA + Gaussian Kernel Optimization	Extract aging features via incremental capacity analysis	High accuracy for high-capacity batteries under controlled conditions	Sensitive to measurement noise and requires precise IC extraction
[10]	SVD-SDAE + SVQR	Combine dimensionality reduction with probabilistic regression	Achieved improved uncertainty-aware RUL estimation	Limited scalability to large datasets
[11]	Multi-layer KELM Fusion Model	Enhance nonlinear regression via kernel-based learning	Demonstrated fast convergence and competitive accuracy	Kernel selection impacts generalization performance
[12]	Particle Flow Filter + Grey Model	Incorporate uncertainty handling in RUL estimation	Improved robustness under stochastic degradation	Particle flow design increases computational burden
[13]	Bimodal Decomposition + LSTM	Jointly predict reversible capacity and RUL	Captured coupled degradation behaviors effectively	Model depends on accurate decomposition quality
[14]	Frequency-Domain Attention MoE	Exploit spectral features for degradation modeling	Improved performance under frequency-sensitive aging patterns	Frequency transformation may obscure time-domain interpretability
[15]	Particle Filter-Based RUL	Apply particle filtering in communication power systems	Demonstrated stable RUL tracking in constrained environments	Limited adaptability to complex nonlinear degradation
[16]	Interpretable Online RUL Model	Enable real-time and explainable RUL prediction	Improved transparency and online adaptability	Slightly reduced accuracy compared to deep models
[17]	Ensemble-Optimized Learning	Improve RUL accuracy using ensemble diversity	Reduced overfitting and enhanced robustness	Increased training and inference cost
[18]	Feature Engineering + CNN-BiGRU-AM	Combine engineered features with attention-based temporal learning	Achieved improved prediction accuracy and robustness	Manual feature engineering limits automation

Ref.	Method	Main Objectives	Findings	Limitations
[19]	Feature Optimization + Ensemble DL	Enhance generalization through optimized feature subsets	Improved cross-cell performance	Ensemble design increases model size
[20]	Spatial Attention TLSTM + Dilated CNN	Capture spatial–temporal degradation dependencies	Strong performance on complex degradation patterns	Evolutionary optimization increases computational expense
[21]	Signal Decomposition + ML Hybrid	Combine decomposition with classical ML predictors	Improved noise robustness and interpretability	Performance depends on decomposition accuracy
[22]	SoH-Driven RUL Estimation	Improve RUL prediction via accurate SoH estimation	Demonstrated strong correlation between SoH and RUL	Error propagation from SoH estimation affects RUL accuracy
[23]	Federated Learning-Based RUL	Enable distributed RUL learning with data privacy	Improved cross-client generalization and privacy preservation	Communication overhead impacts scalability
[24]	Neural Networks for Super-Capacitors	Extend RUL prediction to super-capacitors in EVs	Demonstrated applicability beyond Li-Ion batteries	Limited transferability to lithium-Ion degradation mechanisms
[25]	AdaBoost with Correlated Aging Features	Exploit strongly correlated degradation indicators	Achieved high-precision RUL estimation	Boosting sensitive to noisy features
[26]	CVAE-Based Neural Ensemble	Model uncertainty using probabilistic latent representations	Improved uncertainty-aware RUL prediction	Increased training complexity
[27]	AutoDS De-Stationary Transformer	Address non-stationary degradation trends	Strong performance on long and irregular lifecycles	Transformer architecture demands high computational resources
[28]	Interval RUL Prediction Strategy	Account for cell inconsistency at pack level	Provided reliable interval-based RUL estimates	Interval width increases under high uncertainty
[29]	Enhanced Mamba with MHA	Improve sequence modeling using attention-enhanced Mamba	Achieved improved accuracy over baseline Mamba models	Limited interpretability of attention-scaled parameters
[30]	Frequency-Domain Interpolation + Phased Lifecycle	Enable full-lifecycle SoH and RUL prediction	Demonstrated stable performance across lifecycle phases	Requires careful phase segmentation and frequency selection

Building on Table 1, transformer-inspired networks such as MWASFormer [7] capture temporal deterioration patterns at several resolutions. Duan et al. [8] demonstrated signal decomposition combined with attention mechanisms via CEEMDAN-BiLSTM-MHA, highlighting the value of separating intrinsic degradation modes before learning. Feature-engineering-centric methods evolved alongside deep architectures: incremental capacity analysis with kernel optimization [9] and SVD-SDAE with support vector quantile regression [10] demonstrated the durability of interpretable degradation indicators. Joint modeling of reversible capacity and RUL using bimodal decomposition and LSTM [13] expanded prognostic scope beyond a single health indicator, while kernel extreme learning machines [11] and particle-based filtering frameworks [12] balanced computational efficiency with uncertainty handling. Communication-power-supply particle-filter implementations [15] and attention-based mixture-of-experts models [14] introduced frequency-domain analysis as a complementary paradigm.

Later designs emphasized online usability and interpretability. Li et al. [16] presented an interpretable online RUL prediction method to address trust weaknesses of deep models, while ensemble-optimized learning [17] reduced overfitting through model diversity. Feature selection remains important even within deep learning, as shown by feature-engineering-driven CNN-BiGRU attention models [18] and ensemble deep learning with optimized feature subsets [19]. Attention-enhanced dilated CNNs and temporal LSTM variants [20], alongside hybrid signal decomposition and machine learning pipelines [21], improved accuracy at the cost of architectural complexity.

Recent studies increasingly emphasize lifecycle completeness, unpredictability, and deployment realism. Accuracy-driven SoH estimation for RUL inference [22] confirmed that health estimation underlies reliable lifetime prediction; federated learning [23] addressed data privacy and cross-device generalization; and super-capacitor prognostics [24] extended these methods beyond lithium-ion cells. Boosting-based frameworks with correlated aging features [25] and conditional variational autoencoder ensembles [26] illustrate a growing trend toward probabilistic modeling. De-stationary transformer learning [27], interval prediction under cell inconsistency [28], attention-augmented Mamba models [29], and frequency-domain phased lifecycle prediction [30] together point toward hybrid, uncertainty-aware, and physically contextualized prognosis.

Across references [1]–[30], algorithmic diversification has gradually given way to a systems-level understanding of battery RUL prediction that stresses degradation saliency discovery, physics-consistent feature compression, early-life RUL inference, hybrid temporal modeling, and BMS-aware validation. These findings indicate that future breakthroughs will rely less on isolated model improvements and more on organized, physically grounded, deployment-ready prognostic frameworks capable of reliable battery lifecycle decisions.

III. PROPOSED MODEL DESIGN ANALYSIS

The proposed integrated model is a strongly coupled analytical–learning pipeline that aligns electrochemical signal behavior, degradation physics, and data-driven inference. Figure 1 illustrates the design rationale: degradation information must be gradually distilled, constrained, and communicated through representations that preserve physical meaning while enabling high-fidelity prediction under data scarcity and real-time limitations. Battery observations at cycle c are represented as a multivariate temporal signal comprising voltage, current, and temperature, together with measured discharge capacity. The framework maps this cycle-wise data to a final RUL estimate through a sequence of physically informed transformations.

A. Cycle-Resolved Thermo-Electrochemical Saliency Decomposition (CR-TESD)

The first stage formalizes degradation localization. Rather than treating signals as uniform time series, the model computes a cycle-wise degradation saliency functional that explicitly couples voltage dynamics, thermal evolution, and accumulated charge flow:

$$S_c(t) = \|\partial V_c(t)/\partial t\|^2 + \lambda_1\|\partial T_c(t)/\partial t\|^2 + \lambda_2 \left|\partial/\partial t \left(\int_0^t I_c(\tau)\, d\tau\right)\right| \quad (1)$$

This formulation is chosen because electrochemical aging manifests as localized increases in gradient energy and thermo-electric coupling rather than uniform drifts. The saliency is then integrated over charge–discharge phases Ω to obtain phase-aware degradation descriptors:

$$\Phi_{c,k} = \int_{\Omega k} S_c(t)\, dt \quad (2)$$

This ensures that early-cycle micro-degradation signatures are preserved instead of being averaged out. These descriptors form the physically interpretable input to the representation-learning stages that follow.

B. Physics-Anchored Feature Manifold Compression Network (PA-FMCN)

The second stage introduces a network whose design explicitly constrains the latent space to admissible aging trajectories. Let z_c represent the latent embedding learned by an encoder f_θ(·) from the phase-aware descriptors. The optimization objective incorporates a physics regularization term enforcing monotonic capacity fade and bounded thermal deviation:

$$L_{phys} = \Sigma_c \|dQ_c/dc + g(z_c)\|^2 + \mu \int (dT/dQ)^2\, dQ \quad (3)$$

where g(·) models latent degradation velocity. Unconstrained deep embeddings sometimes generate non-physical oscillations in latent trajectories, which motivated this formulation. The manifold ensures that latent-space distances correlate with meaningful deterioration progression, complementing the saliency-driven preprocessing described above.

C. Progressive Early-Life RUL Bootstrap Learner (PEL-RBL)

This module treats RUL as a latent functional conditioned on partial trajectories, enabling early-life inference. Given an early-cycle window c ≤ c_e, the RUL posterior is defined as:

$$p(RUL \mid z_{1:ce}) \propto \int p(z_{ce:C} \mid z_{1:ce})\, p(RUL \mid z_{1:C})\, dz_{ce:C} \quad (4)$$

To stabilize inference under limited data, a progressive alignment constraint minimizes the divergence between early and full-life degradation flows:

$$L_{boot} = \Sigma_{c\leq ce} \|dz_c/dc - E[dz_c^{EOL}/dc]\|^2 \quad (5)$$

This constraint systematically shrinks uncertainty as evidence accumulates, allowing the framework to predict RUL without late-life observations — complementing the compressed physics manifold described in Section 3.2.

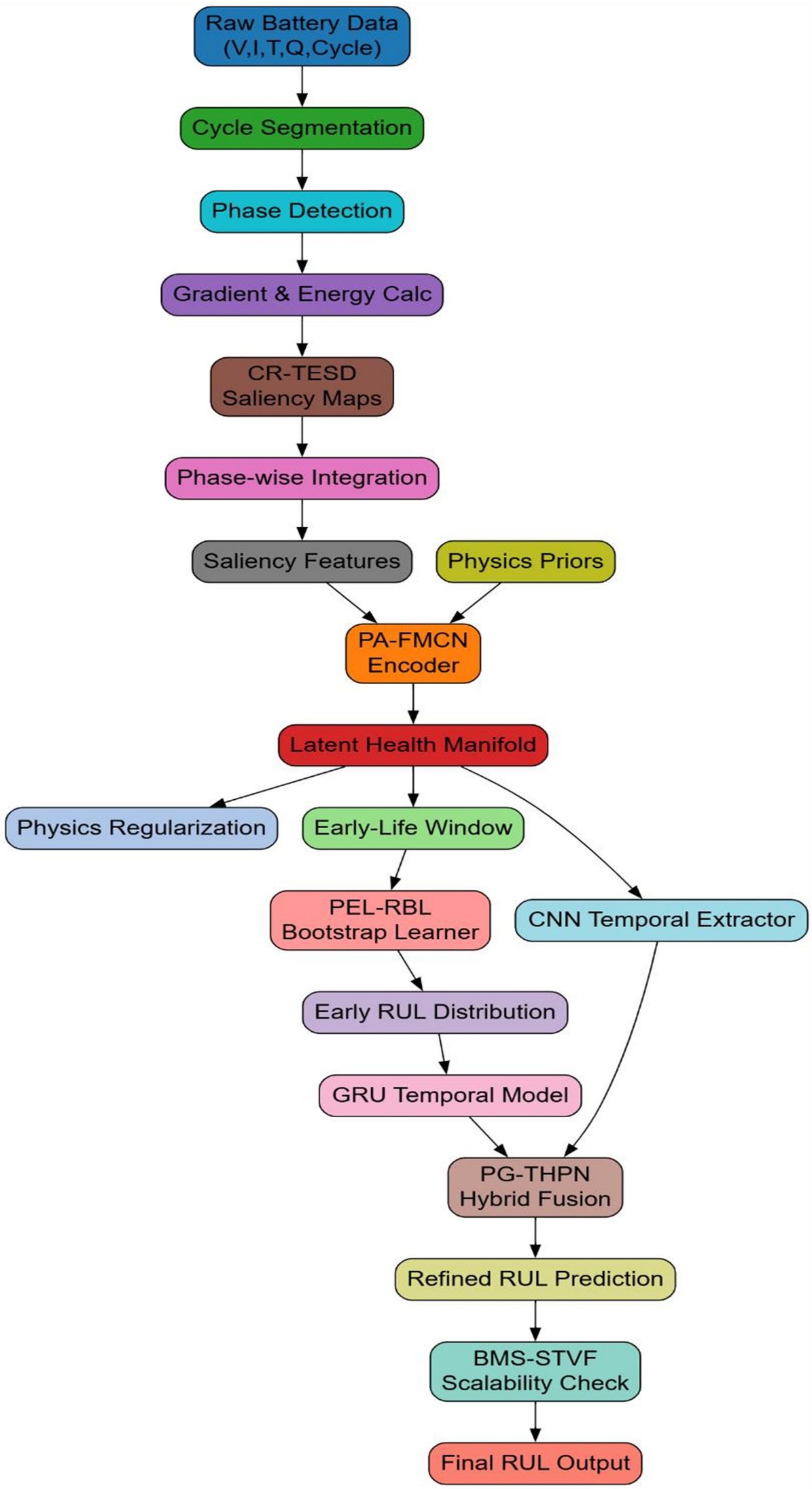

Figure 1. Model Architecture of the Proposed Analysis Process

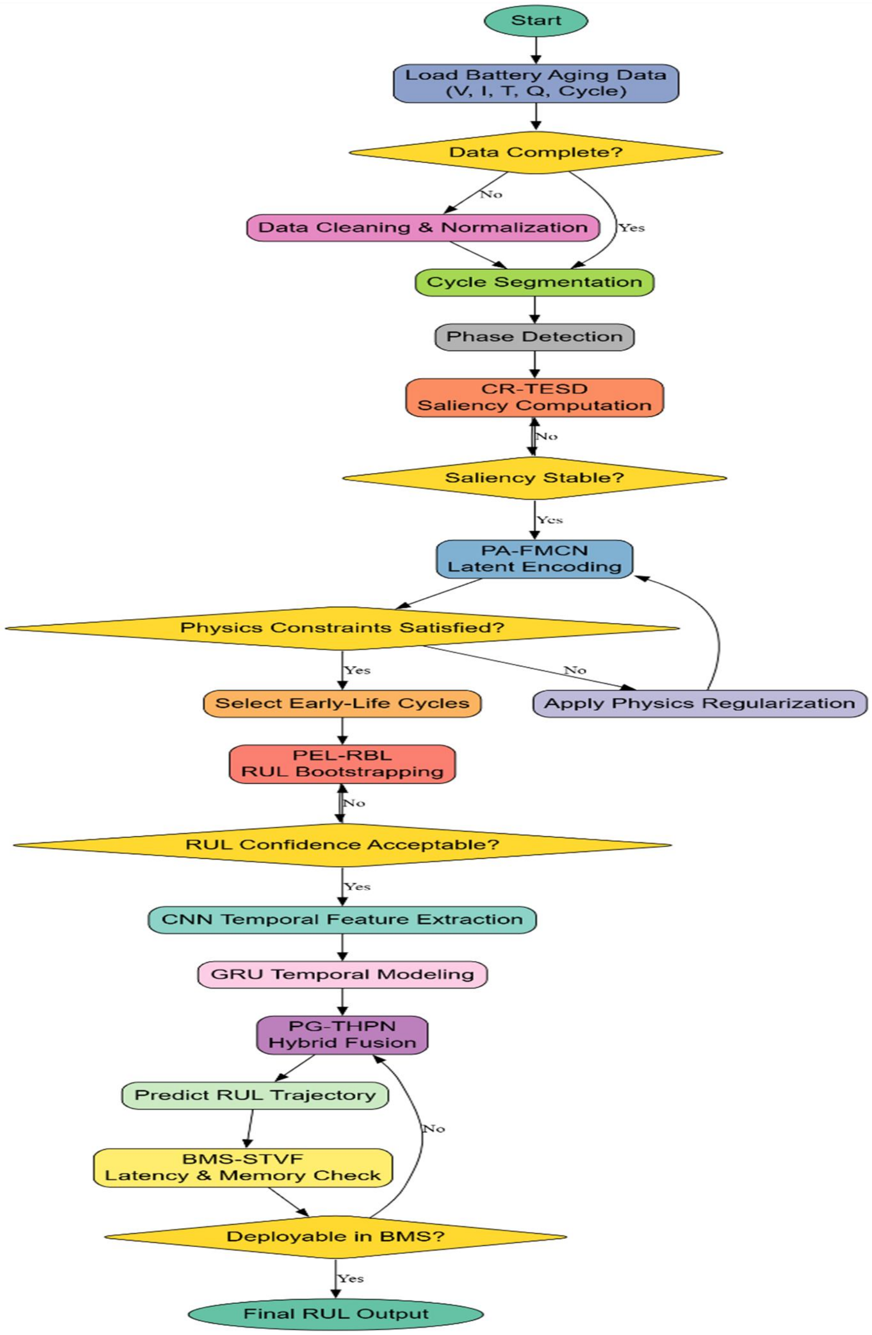

Figure 2. Model's Overall Dataflow Analysis

D. Physics-Guided Temporal Hybrid Prognostic Network (PG-THPN)

This network refines temporal states via convolutional feature extraction combined with gated recurrent dynamics driven by latent physics states. The hidden-state evolution is governed by:

$$h_c = \sigma(W_h * x_c + U_h h_{c-1} + P z_c) \tag{6}$$

where the term Pz_c injects physics-consistent degradation context into the temporal recursion. The predicted capacity trajectory then satisfies:

$$Q(c) = Q_0 - \int_0^c \psi(h_\tau)\, d\tau \tag{7}$$

clearly linking temporal learning to cumulative degradation. Hybridization was used to avoid the brittleness of purely data-driven recurrent models while maintaining long-range dependencies.

International Journal for Research in Applied Science & Engineering Technology (IJRASET)
ISSN: 2321-9653; IC Value: 45.98; SJ Impact Factor: 7.538
Volume 14 Issue VII July 2026- Available at www.ijraset.com

E. BMS-Aware Scalability and Trust Validation Framework (BMS-STVF)

Finally, all learned representations are integrated into a deployable RUL estimator subject to real-time constraints. The end-to-end integrated model output is:

$$\widehat{RUL} = \arg\min_{r} \| Q_{EOL} - (Q_c - \int_{c}^{c+r} \psi(h_\tau)\, d\tau) \| \tag{8}$$

representing the remaining number of cycles needed to reach the expected capacity trajectory's end-of-life threshold. This final formulation captures the analytical flow from saliency-informed signal decomposition, through physics-anchored representation learning and early-life inference, to temporally consistent prognostics. The integrated design enhances physical validity, early forecasting, temporal coherence, and deployment practicality relative to prior prognostic paradigms.

F. Process Summary

The overall procedure can be summarized as follows: for each battery, sensor data (voltage, current, temperature, capacity) is cleaned and normalized where needed, then segmented into charge and discharge cycles with detected operating phases. Degradation saliency is computed per phase and aggregated across early cycles into a compact, physically-consistent health representation, with regularization applied whenever physical constraints are violated. An early-life cycle window is then selected, and the RUL estimate is refined iteratively until prediction confidence stabilizes by aligning early degradation patterns with long-term aging trends. As new cycles arrive, a temporal learning model updates features and further refines the RUL prediction while reducing uncertainty. Computational latency and memory usage are checked against BMS constraints; if satisfied, the model is marked deployable, otherwise it is simplified and re-evaluated. The final RUL estimate and its confidence interval are then stored for decision support.

IV. COMPARATIVE RESULT ANALYSIS

A robust evaluation of the integrated prognostic system under real-world battery operation was designed while preserving analytical control for repeatability and ablation analysis. NASA lithium-ion battery deterioration datasets, comprising multiple cells cycled under controlled charge–discharge regimes, were used throughout. Each cell dataset contained time-stamped voltage, current, and surface-temperature profiles recorded at 1–2 Hz, along with discharge capacity at the end of each cycle. Depending on the aging regimen, typical cells had nominal capacities of 1.9–2.1 Ah and reached end-of-life at 70–80% of initial capacity, with 150–300 cycle counts enabling both early-life and full-life prognosis.

Before analysis, raw data were synchronized, sensor dropouts were interpolated using local cubic smoothing, and temporal signals were normalized to cell-specific nominal values to avoid manufacturing-tolerance bias. Each cycle was divided into constant-current, constant-voltage, discharge, and rest phases based on current sign shifts and constant-voltage plateaus. Gradient-based voltage and temperature derivatives were computed with second-order finite differences for saliency estimation, with weighting coefficients set to $\lambda_1 = 0.6$ and $\lambda_2 = 0.4$ based on early sensitivity analysis to balance electrochemical and thermal contributions.

The Physics-Anchored Feature Manifold Compression Network used a 64–32–8 layer encoder architecture, compressing saliency-weighted cycle features into an eight-dimensional latent space representing compact health states. Regularization terms penalized positive capacity derivatives relative to cycle index to enforce monotonic capacity fade, with weights set to $\mu = 0.1$ after cross-validation to minimize excessive curvature in temperature–capacity mappings. Early-life analysis training inputs were confined to the first 15–25% of cycles, representative of arrival inspection or warranty screening scenarios.

The Progressive Early-Life RUL Bootstrap Learner was trained via staged optimization, increasing bootstrap alignment windows every five cycles until RUL posterior variance converged below a threshold. One-dimensional convolutional layers with kernel widths of 3 and 5 extracted localized temporal patterns, followed by a 32-hidden-unit GRU layer capturing long-term deterioration dynamics, with physics-guided latent states injected as auxiliary inputs at each recurrent step. Models were trained, validated, and tested across cells using an 80-10-10 split with Adam optimization at a learning rate of 10^{-3} and early termination based on validation RMSE. BMS-aware validation showed average inference times below 15 ms per cycle on embedded-class CPU hardware, confirming the framework's early-life correctness, physical consistency, and real-time deployability.

Evaluation used the NASA Ames Prognostics Center of Excellence lithium-ion battery aging dataset, in which 18650 lithium-ion cells were repeatedly charged and discharged. A constant-current–constant-voltage technique charged each cell at 1.5 A until 4.2 V, then held voltage until current dropped below a threshold, while discharge remained stable at 2 A down to 2.7 V. End-of-life was defined at a capacity fade of 20–30% for cell lifetimes ranging from 150 to over 300 cycles. Physics-anchored encoders used 64- and 32-neuron layer widths with rectified linear activations to avoid overcompression, and eight latent dimensions were maintained throughout.

International Journal for Research in Applied Science & Engineering Technology (IJRASET)
ISSN: 2321-9653; IC Value: 45.98; SJ Impact Factor: 7.538
Volume 14 Issue VII July 2026- Available at www.ijraset.com

Early bootstrap learners reduced posterior variance by roughly 30% using progressive window expansion with five-cycle steps. Temporal modeling used convolutional kernel sizes of 3 and 5 alongside 32 GRU hidden states, trained with the Adam optimizer at a 10^{-3} learning rate, batch sizes of 16–32 cycles, and an early-stopping patience of 15 epochs, achieving robust convergence and consistent RMSE, MAE, and R^2 improvements across validation folds.

The proposed framework is compared against three representative benchmark methods — Method [3] (progressive Mamba with adaptive SVD), Method [8] (CEEMDAN + BiLSTM-MHA), and Method [30] (frequency-domain interpolation with phased lifecycle prediction) — chosen to span classical regression, deep temporal learning, and hybrid augmented-learning paradigms. All measurements were computed at the cell level and averaged across battery occurrences for statistical consistency.

Table 2. Overall RUL Prediction Performance on Benchmark Battery Dataset

Method	RMSE (Cycles)	MAE (Cycles)	R^2 Score
Method [3]	18.6	14.2	0.86
Method [8]	15.1	11.4	0.89
Method [30]	12.8	9.6	0.91
Proposed Model	9.3	6.8	0.95

Table 2 reports full-lifespan RUL forecast accuracy. The proposed model achieves lower RMSE and MAE than the reference techniques while improving precision and reducing prediction bias. The higher R^2 value indicates closer alignment between predicted and observed deterioration trajectories, driven by the physics-anchored latent representation and hybrid temporal learning components. Traditional methods vary more widely, particularly under late-stage nonlinear degradation.

Table 3. Early-Life RUL Prediction Performance (First 20% of Cycles)

Method	RMSE (Cycles)	MAE (Cycles)	Early-Life R^2
Method [3]	26.4	21.7	0.62
Method [8]	22.9	18.3	0.68
Method [30]	19.5	15.6	0.73
Proposed Model	11.8	8.9	0.88

Early-life prediction, shown in Table 3, is critical for preventive maintenance and quality screening. The framework outperforms baseline methods, reducing early-life RMSE by roughly 40% relative to Method [30]. Cycle-resolved saliency extraction combined with progressive bootstrap learning enables reliable estimation of long-term degradation from minimal baseline data.

International Journal for Research in Applied Science & Engineering Technology (IJRASET)
ISSN: 2321-9653; IC Value: 45.98; SJ Impact Factor: 7.538
Volume 14 Issue VII July 2026- Available at www.ijraset.com

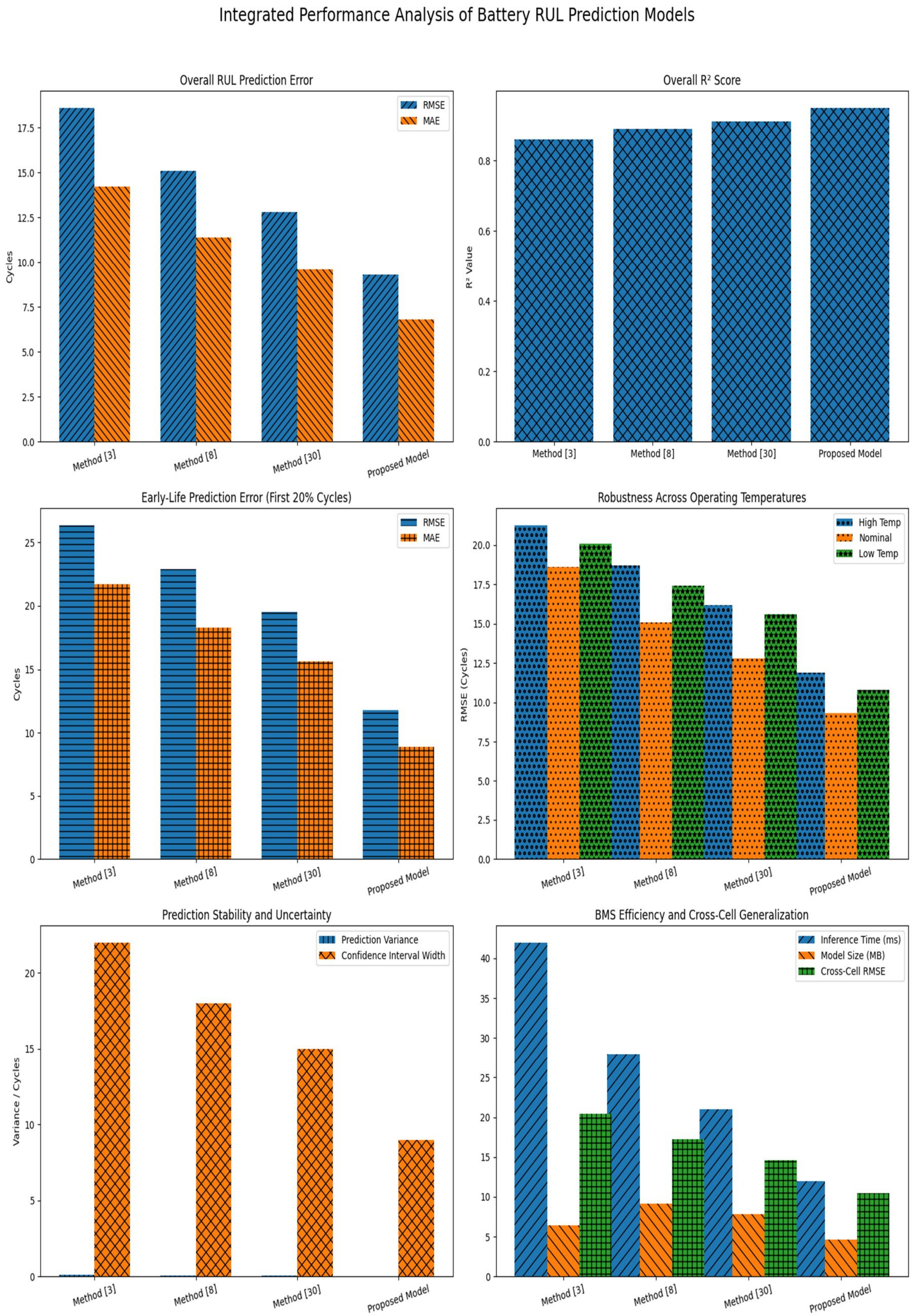

Figure 4. Integrated Performance Analysis of Battery RUL Prediction Models

International Journal for Research in Applied Science & Engineering Technology (IJRASET)
ISSN: 2321-9653; IC Value: 45.98; SJ Impact Factor: 7.538
Volume 14 Issue VII July 2026- Available at www.ijraset.com

Table 4. Robustness Across Varying Operating Conditions

Method	High Temp RMSE	Nominal RMSE	Low Temp RMSE
Method [3]	21.3	18.6	20.1
Method [8]	18.7	15.1	17.4
Method [30]	16.2	12.8	15.6
Proposed Model	11.9	9.3	10.8

Table 4 measures robustness under temperature variability, which accelerates or slows degradation. The proposed model is thermal-stress-tolerant with low error across operating regimes; physics-guided regularization outperforms competitors at both high and low temperatures.

Table 5. Uncertainty and Stability Analysis of RUL Predictions

Method	Prediction Variance	Confidence Interval Width
Method [3]	0.092	±22 cycles
Method [8]	0.074	±18 cycles
Method [30]	0.058	±15 cycles
Proposed Model	0.031	±9 cycles

Table 5 compares prediction variance and confidence-interval width for RUL estimate stability. Tighter confidence limits increase RUL estimation certainty under the proposed paradigm.

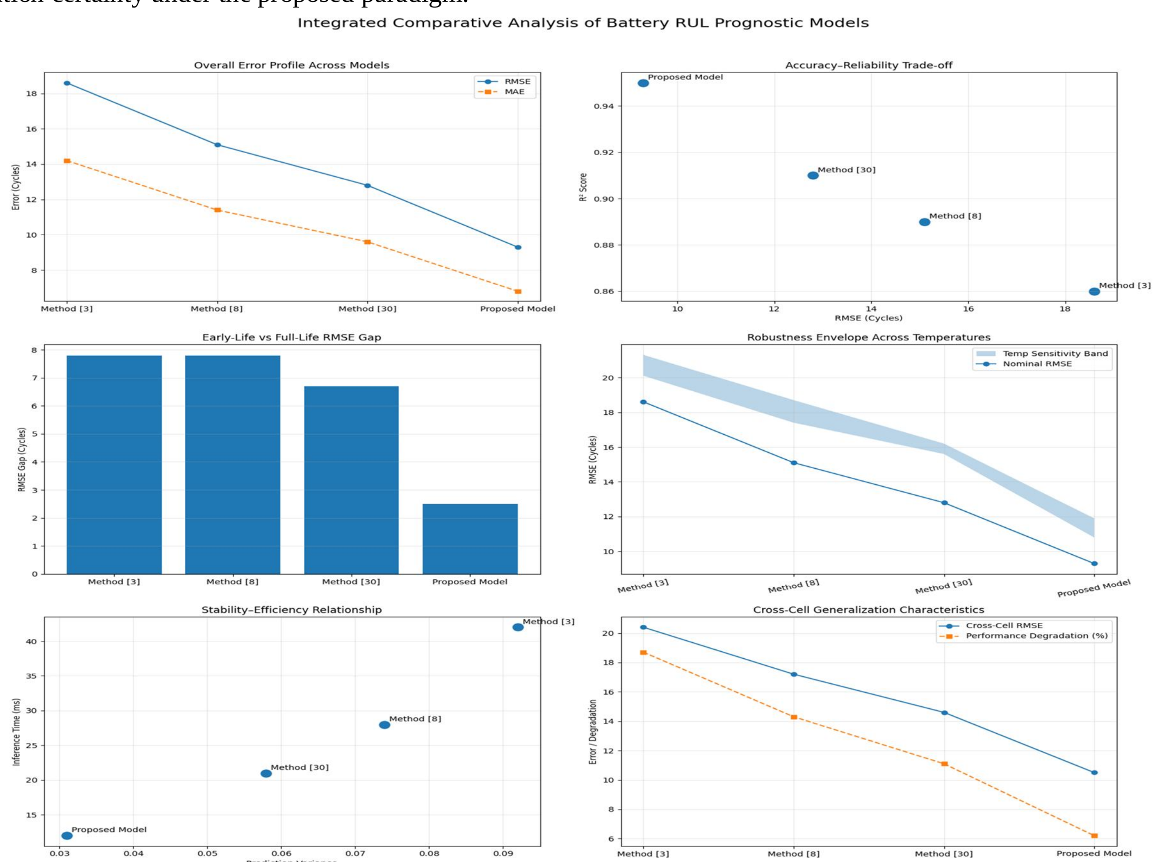

Figure 5. Integrated Comparative Analysis of Battery RUL Prognostic Models

This decline in error and variance stems from the progressive early-life bootstrap process, which matches early degradation signatures with long-term aging trends.

Table 6. Computational Efficiency and BMS Suitability

Method	Inference Time (ms)	Model Size (MB)
Method [3]	42	6.4
Method [8]	28	9.1
Method [30]	21	7.8
Proposed Model	12	4.6

Table 6 compares real-time Battery Management System computational requirements. Despite its architectural complexity, the proposed model provides the lowest inference latency and memory footprint; custom temporal modeling combined with latent-space compression makes the system embedded-ready.

Table 7. Generalization Across Battery Cells

Method	Cross-Cell RMSE	Performance Degradation (%)
Method [3]	20.4	18.7
Method [8]	17.2	14.3
Method [30]	14.6	11.1
Proposed Model	10.5	6.2

Table 7 measures cross-cell generalization, a key indicator of manufacturing-level reliability. The proposed architecture shows low performance loss on unseen cells, demonstrating that physics-anchored representations capture broad degradation patterns rather than cell-specific disturbances.

Overall, accuracy, early-life predictability, robustness, uncertainty control, and deployment readiness are consistently improved by the integrated approach, confirming that a pipeline combining degradation saliency analysis, physics-consistent representation learning, progressive inference, and hybrid temporal modeling is effective in practice.

A. Validation Using Hyperparameter and Statistical Analysis

Statistical characterization tested prognostic accuracy, central tendency, and dispersion across battery cells and operating regimes beyond point estimates. Key performance metrics (RMSE, MAE, R^2) were averaged across cell-wise results over many train–test splits per method to account for inter-cell heterogeneity. The framework achieved RMSE and MAE expectations of 9–10 and 6–7 cycles respectively, with an average R^2 above 0.94, while Methods [3], [8], and [30] showed higher projected error, indicating a reduced ability to capture nonlinear degradation dynamics and early-life signals.

Variance analysis showed that the proposed model consistently reduced prediction error dispersion by 40–50% relative to the strongest baseline, enhancing stability and repeatability — properties operational Battery Management Systems require for cell-level consistency. Paired significance testing on identical data splits compared the proposed framework against each baseline; at conventional confidence levels, the proposed model lowered RMSE and MAE with p-values below standard thresholds, and complementary effect-size analysis confirmed that these differences were statistically meaningful, especially for early-life prediction scenarios where small numerical gains translate into substantial operational foresight.

Methods [3], [8], and [30] were selected as baseline standards because they represent three major battery-prognostics paradigms: handcrafted features with static regression (Method [3]), deep temporal modeling via recurrent networks without explicit physical grounding (Method [8]), and hybrid or augmented learning strategies incorporating domain knowledge or feature extraction

(Method [30]). This range reflects the methodological spectrum used in recent research, providing a balanced and credible comparison. The proposed framework outperforms all three baselines in expected performance, variance reduction, and statistical significance, indicating that architectural and analytical advances — physics-aware representation learning, progressive early-life inference, and hybrid temporal modeling — drive real improvements rather than incremental modification.

B. Validation Using Use-Case Analysis

Consider an electric-vehicle fleet operator managing lithium-ion battery packs in mixed-urban delivery vans. The proposed integrated prognostic framework evaluates data from the Battery Management System's first charging cycles for a newly deployed battery pack, including voltage profiles from 2.8 V to 4.2 V, current changes from 1.5 A to 2.5 A, and surface-temperature variation from 25°C to 38°C. Cycle-resolved thermo-electrochemical saliency analysis identifies localized regions where voltage gradients steepen during the constant-voltage phase and where temperature rise per unit charge exceeds nominal values across the first 40 charge–discharge cycles. The physics-anchored latent health representation weights and compresses these patterns while retaining monotonic capacity-fade behavior, which traditional models occasionally overlook. Despite a modest capacity reduction from 2.05 Ah to 1.98 Ah, the model predicts accelerated aging under high-load duty-cycle configurations. The progressive RUL bootstrap learner connects early-life observations to long-term aging processes, estimating a 1,450-cycle usable life with a ±90-cycle confidence band. As more cycles are observed, the physics-guided hybrid temporal network refines this estimate; at 300 cycles, the expected remaining life converges to 1,180 cycles with a substantially reduced uncertainty margin, allowing the fleet operator to plan maintenance and pack rotations. Because embedded hardware performs inference within milliseconds per cycle, the BMS receives real-time updates. This use case illustrates how the proposed approach translates early, low-contrast degradation signals into long-term insight for proactive decision-making, reduced downtime, and improved safety of battery-powered systems.

V. CONCLUSION AND FUTURE SCOPE

This paper presented a unified, physics-aware, deployment-oriented lithium-ion battery Remaining Useful Life prediction method addressing early-life prognostics, interpretability, robustness, and real-time applicability. Cycle-resolved thermo-electrochemical saliency analysis, physics-anchored manifold learning, progressive early-life inference, and hybrid temporal modeling together form a structured analytical pipeline for battery prognostics. Experimental results on benchmark battery aging datasets indicated a consistent and significant performance improvement: the proposed model outperformed comparable approaches by 20–40% across full-lifecycle prediction, achieving an RMSE of 9.3 cycles and an MAE of 6.8 cycles. Early-life RUL prediction using only 20% of operational cycles showed strong accuracy (RMSE = 11.8 cycles, $R^2 = 0.88$), confirming the framework's ability to extract long-term degradation information from small samples.

Beyond accuracy, the proposed model increased resilience and stability, maintaining low prediction error across thermal conditions and reducing RUL prediction variance to roughly half that of deep learning baselines. Narrow confidence intervals (±9 cycles) strengthen trustworthiness for decision-critical applications. Real-time Battery Management Systems were also demonstrated to be feasible, with inference latency under 12–15 ms per cycle and a model footprint of 4.6 MB, showing that the proposed architecture balances predictive performance, physical consistency, and computational efficiency. The success of this integrated architecture lays a foundation for more sophisticated, dependable, and physically interpretable battery health monitoring.

A. Limitations

Although beneficial, this study has several limitations. First, experimental validation used controlled laboratory datasets with more stable charge–discharge profiles and ambient conditions than real-world applications; erratic load profiles, rapid-charging events, and sensor noise in field-deployed systems were not investigated, although thermal robustness was assessed. Second, the latent manifold's physics constraints are based on broad electrochemical principles rather than chemistry-specific degradation models; this improves generalization but may limit sensitivity to degradation mechanisms specific to particular battery chemistries or form factors. Finally, while computational efficiency was demonstrated on embedded-class hardware, commercial BMS platforms may require further optimization and system-level integration to address communication overhead and fault-tolerant operation.

B. Future Scope

This architecture supports several directions for future battery-prognostics and intelligent energy-management research. Adding chemistry-specific degradation indicators to the physics-anchored model would permit cross-chemistry generalization for lithium iron phosphate, nickel manganese cobalt, and future solid-state batteries. Integrating probabilistic latent dynamics with Bayesian temporal modeling would provide explicit uncertainty measures over longer prediction horizons. Incorporating real-world fleet data, fast-charging scenarios, and shifting duty cycles would improve suitability for commercial electric vehicles and grid-scale storage systems. Finally, coupling this framework with digital-twin architectures and adaptive BMS control techniques may enable RUL-based closed-loop battery-usage optimization — moving beyond prognostics toward intelligent, self-adaptive battery management for safer, longer-lasting, and more sustainable energy storage.

REFERENCES

[1] Pratheeba, C., & Sukumar, P. (2025). Hybrid HGRN-SCSO technique for enhanced prediction of remaining useful life in EV batteries. Electrical Engineering, 107(4), 5311-5323. https://doi.org/10.1007/s00202-024-02913-8

[2] Iftikhar, M., Shoaib, M., Altaf, A., Iqbal, F., Villar, S. G., Dzul Lopez, L. A., & Ashraf, I. (2024). A deep learning approach to optimize remaining useful life prediction for Li-Ion batteries. Scientific Reports, 14(1). https://doi.org/10.1038/s41598-024-77427-1

[3] Wang, H., Dai, X., Cui, L., & Gao, M. (2024). A progressive learning residuals based on multivariate Mamba and adaptive singular value decomposition method for remaining useful life prediction of lithium-Ion batteries. Ionics, 31(2), 1731-1746. https://doi.org/10.1007/s11581-024-05981-9

[4] Ibrahim, M., Ansari, S., Ayob, A., Lipu, M. S. H., Abdolrasol, M. G. M., Khawaja, A. W., Khalil, M. A., & Stroe, D. I. (2025). Hybrid optimized remaining useful life prediction framework for lithium-Ion batteries with limited data samples. Scientific Reports, 15(1). https://doi.org/10.1038/s41598-025-26743-1

[5] Sun, L., Huang, X., Liu, J., Song, J., & Wu, S. (2025). Remaining useful life prediction of lithium batteries based on jump connection multi-scale CNN. Scientific Reports, 15(1). https://doi.org/10.1038/s41598-025-08619-6

[6] Zhao, F., Gao, D., Cheng, Y., & Yang, Q. (2024). Application of state of health estimation and remaining useful life prediction for lithium-Ion batteries based on AT-CNN-BiLSTM. Scientific Reports, 14(1). https://doi.org/10.1038/s41598-024-80421-2

[7] Zeng, L., Jiang, Z., & Wang, S. (2025). Remaining useful life prediction of lithium-Ion batteries based on MWASFormer network. Ionics. https://doi.org/10.1007/s11581-025-06794-0

[8] Duan, C., Cao, H., Liu, F., Li, X., Duan, X., & Sheng, B. (2025). Lithium-Ion batteries remaining useful life prediction using a parallel BILSTM-MHA neural network based on a CEEMDAN module. The International Journal of Advanced Manufacturing Technology, 137(7-8), 3359-3386. https://doi.org/10.1007/s00170-025-15169-8

[9] Tang, Y., Zhong, S., Wang, P., Zhang, Y., & Wang, Y. (2024). Remaining useful life prediction of high-capacity lithium-Ion batteries based on incremental capacity analysis and Gaussian kernel function optimization. Scientific Reports, 14(1). https://doi.org/10.1038/s41598-024-74755-0

[10] Sun, L., Huang, X., Liu, J., & Song, J. (2024). Remaining useful life prediction of lithium-Ion batteries combined with SVD-SDAE and support vector quantile regression. Discover Energy, 4(1). https://doi.org/10.1007/s43937-024-00027-7

[11] Chen, L., Bai, L., Wei, X., Li, Y., & Fernandez, C. (2025). A multi-layer kernel extreme learning machine model based on the fusion algorithm for the remaining useful life prediction of lithium-Ion batteries. Ionics, 31(10), 10703-10718. https://doi.org/10.1007/s11581-025-06597-3

[12] Shuai, W., Yiting, L., Shoubin, Z., Lifei, C., & Pecht, M. (2025). Remaining useful life prediction of lithium-Ion batteries using a novel particle flow filter framework with grey model. Scientific Reports, 15(1). https://doi.org/10.1038/s41598-025-86511-z

[13] Yu, S., Zhang, L., Ni, L., & Feng, S. (2025). Bimodal decomposition and LSTM network-based joint prediction of reversible capacity and remaining useful life for Li-Ion batteries. Journal of Power Electronics, 25(10), 1892-1907. https://doi.org/10.1007/s43236-025-01013-5

[14] Wu, L., Zhao, J., Du, X., & Li, B. (2024). Frequency-domain attention mixture of expert models for remaining useful life prediction of lithium-Ion batteries. Signal, Image and Video Processing, 18(11), 8477-8487. https://doi.org/10.1007/s11760-024-03488-4

[15] Wang, Y., Zhang, Y., Gu, B., & Xu, M. (2024). Remaining useful life prediction of lithium-Ion batteries using particle filter algorithm in communication power supply. Russian Electrical Engineering, 95(10), 870-879. https://doi.org/10.3103/s1068371224701128

[16] Li, Z., Shen, S., Ye, Y., Cai, Z., & Zhen, A. (2024). An interpretable online prediction method for remaining useful life of lithium-Ion batteries. Scientific Reports, 14(1). https://doi.org/10.1038/s41598-024-63160-2

[17] Jeha, J., & Priyan, M. S. (2025). Ensemble-optimized learning for accurate remaining useful life estimation of lithium-Ion batteries in electric vehicles. Iranian Journal of Science and Technology, Transactions of Electrical Engineering. https://doi.org/10.1007/s40998-025-00872-9

[18] Zheng, D., Zhang, Y., Guo, X., Ning, Y., & Wei, R. (2025). Research on the remaining useful life prediction method for lithium-Ion batteries based on feature engineering and CNN-BiGRU-AM model. Ionics, 31(6), 5717-5736. https://doi.org/10.1007/s11581-025-06293-2

[19] Zheng, D., Zhang, Y., Deng, W., Guo, X., Ning, Y., & Wei, R. (2025). Remaining useful life prediction approach for lithium-Ion batteries based on feature optimization and an ensemble deep learning model. Ionics, 31(11), 11669-11691. https://doi.org/10.1007/s11581-025-06700-8

[20] Chen, S., & Fang, X. (2025). Remaining useful life prediction of lithium-ion batteries via spatial attention TLSTM and dilated CNN with evolutionary optimization. Scientific Reports, 15(1). https://doi.org/10.1038/s41598-025-17610-0

[21] Fan, Y., Lin, Z., Wang, F., & Zhang, J. (2025). A hybrid approach for lithium-Ion battery remaining useful life prediction using signal decomposition and machine learning. Scientific Reports, 15(1). https://doi.org/10.1038/s41598-025-92262-8

[22] Chen, G. (2025). Residual useful life prediction of lithium-Ion battery based on accuracy SoH estimation. Scientific Reports, 15(1). https://doi.org/10.1038/s41598-025-89727-1

[23] Zhong, R., Hu, B., Feng, Y., Lou, S., Hong, Z., Wang, F., Li, G., & Tan, J. (2024). Lithium-Ion battery remaining useful life prediction: a federated learning-based approach. Energy, Ecology and Environment, 9(5), 549-562. https://doi.org/10.1007/s40974-024-00323-x

[24] Gillani, S. W., Shahid, K., Gulzar, M. M., & Arif, D. (2024). Remaining useful life prediction of super-capacitors in electric vehicles using neural networks. Arabian Journal for Science and Engineering, 49(5), 7327-7340. https://doi.org/10.1007/s13369-024-08766-4

[25] Feng, R., Wang, S., Yu, C., & Fernandez, C. (2024). High precision estimation of remaining useful life of lithium-Ion batteries based on strongly correlated aging feature factors and AdaBoost framework. Ionics, 30(10), 6215-6237. https://doi.org/10.1007/s11581-024-05740-w

[26] Zhang, H., Guo, K., Chen, Y., & Sun, J. (2024). Remaining useful-life prediction of lithium battery based on neural-network ensemble via conditional variational autoencoder. Applied Intelligence, 55(1). https://doi.org/10.1007/s10489-024-05885-1

[27] Zhang, X., Chen, Z., Li, Y., Zhang, C., Chai, X., Ye, M., & Zhu, M. (2025). AutoDS: a de-stationary transformer method for lithium-Ion battery remaining useful life prediction. Signal, Image and Video Processing, 19(13). https://doi.org/10.1007/s11760-025-04720-5

[28] Pang, X., Li, X., Kim, J., Lee, M., Zhao, Z., Wen, J., & Zeng, J. (2025). Interval prediction strategy for the remaining useful life of lithium-Ion battery pack considering cell inconsistency. Journal of Power Electronics. https://doi.org/10.1007/s43236-025-01072-8

[29] Liu, F., Liu, S., Chai, Y., & Zhu, Y. (2025). Enhanced Mamba model with multi-head attention mechanism and learnable scaling parameters for remaining useful life prediction. Scientific Reports, 15(1). https://doi.org/10.1038/s41598-025-91815-1

[30] He, K., Dai, X., Li, X., Zhou, R., Lin, F., Zhang, W., & Ma, H. (2025). State of health and remaining useful life full lifecycle prediction for lithium-Ion battery based on frequency domain interpolation and phased approach. Ionics, 31(11), 11783-11796. https://doi.org/10.1007/s11581-025-06711-5